

X-ray micro-CT with a displaced detector array

Ge Wang^{a)}

CT/Micro-CT Lab, Department of Radiology and Department of Biomedical Engineering,
University of Iowa, Iowa City, Iowa 52242

(Received 14 August 2001; accepted for publication 2 May 2002; published 24 June 2002)

Because the sizes of samples differ in x-ray micro-CT applications, it is desirable to have a mechanism to change the field of view of a micro-CT scanner. A well-known way to double the diameter of the field of view is to displace a detector array by 50%. In this paper, we propose to displace a detector array by an amount of greater than 0% but less than 50% for a continuously adjustable field of view, and formulate a weighting scheme for artifact-free reconstruction. Then, we perform numerical simulation with the Shepp–Logan phantom to demonstrate the feasibility in fan-beam and cone-beam geometry. © 2002 American Association of Physicists in Medicine.

[DOI: 10.1118/1.1489043]

Key words: X-ray computed tomography (CT), micro-CT, field of view, fan-beam, cone-beam, image reconstruction

With improvement of x-ray source and detector technologies as well as increasing biomedical needs for micro-CT, there is a great interest in developing micro-CT scanners capable of imaging samples of different sizes. Practically, it is preferred to cover samples of various sizes with a given detector array (for example, a CCD camera). A traditional way for doubling the field of view is to displace a detector array by 50% of the detection range, and rebin truncated data into a set of complete data. To the best of our knowledge, the cases of detector displacement of greater than 0% but less than 50% has not been studied before. In this paper, we first describe the geometry of the detector array displacement, and formulate a data weighting scheme for image reconstruction. Then, we perform numerical simulation with the Shepp–Logan phantom to demonstrate the feasibility of the weighting scheme in fan-beam and cone-beam geometry.

The advantages of such a detector displacement is two-fold. First, more data can be acquired for improved spatial and contrast resolution. Second, data processing for image reconstruction can be performed more efficiently. In contrast to our direct weighting scheme to be described below, traditional rebinning operations would compromise the spatial resolution in the interpolation process. Additionally, the rebinning process is more computationally involved than our weighting scheme.

We illustrate the fan-beam geometry in Fig. 1, where the detector array is scaled to go through the origin of the reconstruction system, β denotes the angular position of an x-ray source, R the source-to-origin distance, t and α are respectively the spatial and angular positions of a detector, Δ and δ the larger spatial and angular spans of the detector array, Θ and θ the corresponding smaller spans of the array. The percentage p of the detector array displacement can be defined as follows:

$$p = \frac{\frac{\Theta + \Delta}{2} - \Theta}{\Theta + \Delta} \times 100\%. \quad (1)$$

Note that p is between 0% and 50%. In Fig. 1, the detector array is displaced along the direction of the t axis to increase the field of view. In the most common equispacial fan-beam geometry, the detector array can be physically displaced, while the source-to-detector distance remains constant. In a scanning process, the detector array will not be repositioned.

It can be shown that the fan-beam imaging with a displaced detector array leads to a rectangular redundant data region, as indicated in gray in Fig. 2. We first give the following weighting function on the rectangular redundant region for equiangular data:

$$w(\alpha, \beta) = \frac{1}{2} \left(\sin\left(\frac{\pi\alpha}{2\theta}\right) + 1 \right), \quad -\theta \leq \alpha \leq \theta. \quad (2)$$

Then, we transform the above formula for equispacial data:

$$w(t, \beta) = \frac{1}{2} \left(\sin\left(\frac{\pi \arctan\left(\frac{t}{R}\right)}{2 \arctan\left(\frac{\Theta}{R}\right)}\right) + 1 \right), \quad -\Theta \leq t \leq \Theta. \quad (3)$$

The above weighting scheme can be visualized in Fig. 3. It is straightforward to verify that the weighting scheme does meet all the requirements imposed by Parker,¹ i.e., (1) boundary continuity and (2) unit total weight over the rectangular redundancy region. Specifically, because the sine function and its derivatives are continuous, we immediately have the boundary continuity. To show the unit total weight over the redundant region, we utilize the relationship between opposite rays¹ and compute the total weight as follows:

$$\begin{aligned} w(\alpha, \beta) + w(-\alpha, \beta + \pi + 2\alpha) \\ = \frac{1}{2} \left(\sin\left(\frac{\pi\alpha}{2\theta}\right) + 1 \right) + \frac{1}{2} \left(\sin\left(\frac{-\pi\alpha}{2\theta}\right) + 1 \right) = 1. \end{aligned} \quad (4)$$

Similar to what was done with the weighting scheme for

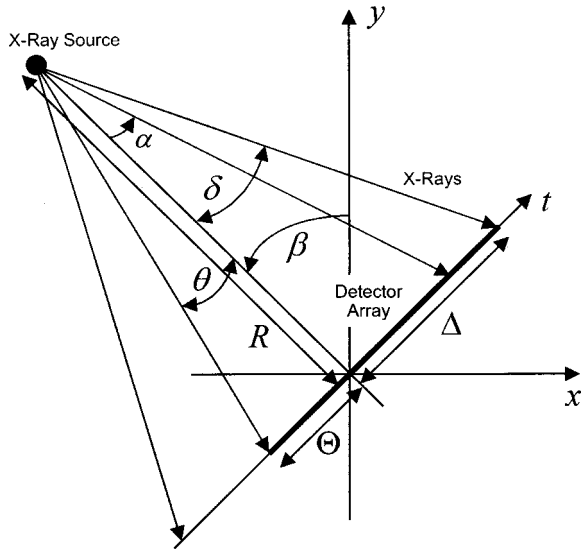


FIG. 1. Fan-beam geometry with a displaced detector array.

multiple x-ray sources,² the above weighting function can be inserted into not only the conventional fan-beam reconstruction formula but also the Feldkamp-type cone-beam reconstruction formula^{3,4} for image reconstruction with a displaced two-dimensional (2-D) detector array:

$$g(x, y, z) = \frac{1}{2} \int_0^{2\pi} \frac{\rho^2(\beta)}{(\rho(\beta) - v)^2} \int_{-\infty}^{\infty} w(p, \beta) D(\beta, p, \zeta) \times f\left(\frac{\rho(\beta)u}{\rho(\beta) - v} - p\right) \frac{\rho(\beta)}{\sqrt{\rho^2(\beta) + p^2 + \zeta^2}} dp d\beta, \quad (5)$$

where $\rho(\beta)$ is the distance between the source and the z axis,

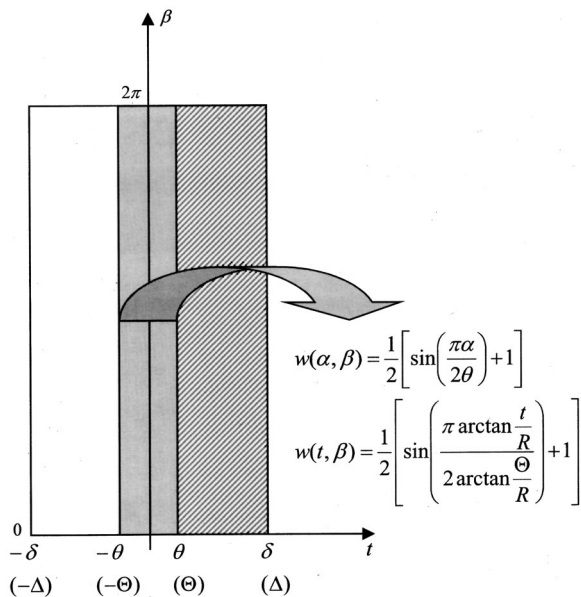


FIG. 2. Redundant region and weighting function for fan-beam CT with a displaced detector array.

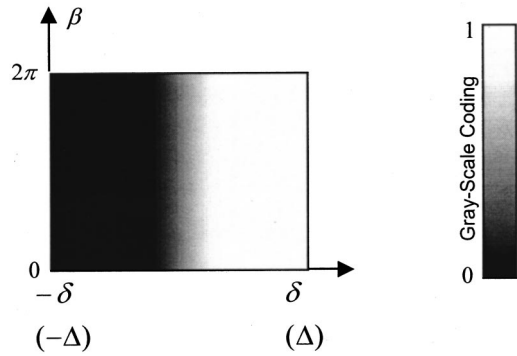


FIG. 3. Illustration of the weighting function for fan-beam CT with a displaced detector array.

$$\zeta = \frac{\rho(\beta)\bar{z}(\beta)}{\rho(\beta) - u}, \quad u = x \cos \beta + y \sin \beta,$$

$$v = -x \sin \beta + y \cos \beta, \quad \bar{z}(\beta) = z - h(\beta),$$

$h(\beta)$ the distance between the source and the x - y plane, $w(p, \beta)$ the weighting function for equispacial data, $D(\beta, p, \zeta)$ equispacial cone-beam data, and $f(\cdot)$ the reconstruction filter.

In our numerical simulation of micro-CT with a displaced detector array, both fan-beam and cone-beam image reconstruction programs were developed in C on an SGI O2 workstation. The 3-D Shepp and Logan phantom was used as the testing object.²

First, we performed the fan-beam simulation. The source-to-origin distance was 5. The length of the detector array was 2.2 with 256 cells. The number of projections was 200. The offsets were about 13% and 27%, respectively. The 2-D phantom was extracted at $z = -0.25$ from the 3-D phantom. Images were reconstructed on 256 by 256 matrices. The pixel values were linearly transformed into 256 discrete gray levels. Figure 4 shows images reconstructed from data collected with the displaced 1-D detector array using either weights of $\frac{1}{2}$ or our proposed weights, along with mean absolute errors.

Then, we performed the cone-beam simulation in a similar fashion. The detector plane was set to 2.2 by 2.2 with 256 by 256 detectors, whose center was at the origin of the reconstruction coordinate system x - y - z . A circular scanning locus of radius 5 was used. The number of projection was also 200. Images were reconstructed on 256 by 256 matrices as well. Figure 5 shows images reconstructed from data collected with the displaced 2-D detector array using the Feldkamp algorithm after either $\frac{1}{2}$ weighting or our proposed weighting, along with mean absolute errors.

It is observed that the images reconstructed using the proposed weighting scheme contain little artifacts, and do not differ visually from the traditional reconstruction. Although with the detector array displacement parts of an object pass outside the field of view, the missing locations in the sinogram will be covered, because the sinogram is doubly sampled during a traditional full scan. Note that the re-

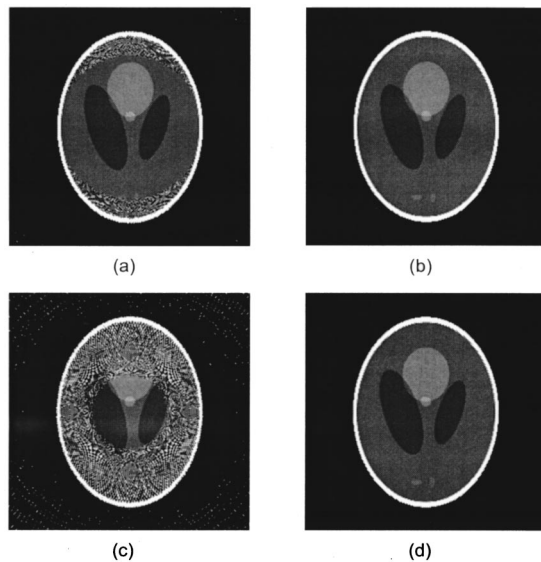


FIG. 4. Numerical simulation of fan-beam CT with a displaced detector array. (a) Reconstruction of the Shepp–Logan phantom with 13% detector displacement and $\frac{1}{2}$ weights; (b) reconstruction of (a) using our proposed weights; (c) Reconstruction with 27% detector displacement and $\frac{1}{2}$ weights, (d) reconstruction of (c) using our proposed weights. Relative to the standard filtered backprojection image, the mean absolute-errors of the images are (a) 4.92, (b) 0.25, (c) 28.56, and (d) 0.27.

relationship between the image quality and the imaging parameters essentially remains the same as what is well known in the field, except that the data sampling density in the sinogram has been decreased with the detector displacement scheme.

We emphasize that although data collected using the displaced detector array can be rebinned for reconstruction, it is advantageous in terms of spatial resolution and computational efficiency to weight the truncated data appropriately then reconstruct images directly from the weighted data. In other words, if the data are not weighted according to a weighting scheme, they must be rebinned to a set of complete data. The interpolation operations needed for rebinning would necessarily blur the sampling resolution. Furthermore, the rebinning-and-reconstruction scheme would be more computationally complex than our weighting-and-reconstruction scheme.

The disadvantages of the detector array displacement include the need for physically displacing the detector array and the asymmetric sampling rates around the isocenter and near the peripheral region. Also, this scheme is not much

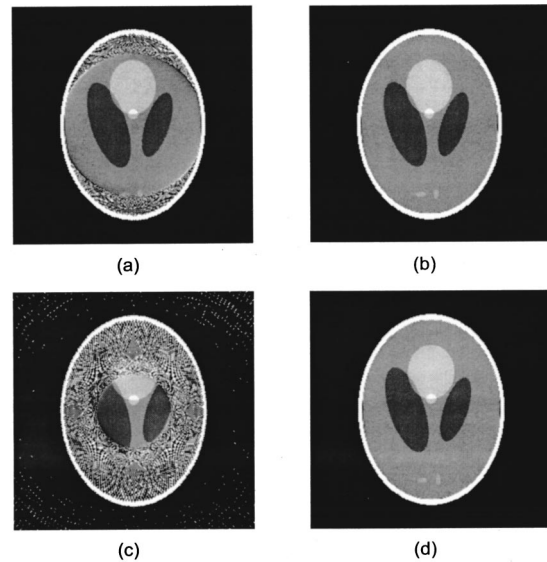


FIG. 5. Numerical simulation of cone-beam CT with a displaced detector array. (a) Reconstruction of the Shepp–Logan phantom with 13% detector displacement and $\frac{1}{2}$ weights; (b) reconstruction of (a) using our proposed weights; (c) Reconstruction with 27% detector displacement and $\frac{1}{2}$ weights, (d) reconstruction of (c) using our proposed weights. Relative to the standard filtered backprojection image, the mean absolute errors of the images are (a) 6.76, (b) 0.57, (c) 30.72, and (d) 0.51.

useful for a medical CT system, since the size of the patient is relatively fixed, and we do not need much flexibility as we do with micro-CT.

In conclusion, we have proposed a flexible scanning mode by displacing a detector array for a continuously adjustable field of view, and formulated a weighting scheme for direct filtered backprojection in fan-beam and cone-beam geometry. This weighting scheme may be applied with other cone-beam algorithms as well.⁵

^a)Electronic mail: ge-wang@uiowa.edu

¹D. L. Parker, "Optimal short scan convolution reconstruction for fan-beam CT," *Med. Phys.* **9**, 254–257 (1982).

²Y. Liu, H. Liu, Y. Wang, and G. Wang, "Half-scan cone-beam CT fluoroscopy with multiple x-ray sources," *Med. Phys.* **28**, 1466–1471 (2001).

³L. A. Feldkamp, L. C. Davis, and J. W. Kress, "Practical cone-beam algorithm," *J. Opt. Soc. Am. A* **1**, 612–619 (1984).

⁴G. Wang, T. H. Lin, P. C. Cheng, and D. M. Shinozaki, "A general cone-beam reconstruction algorithm," *IEEE Trans. Med. Imaging* **12**, 486–496 (1993).

⁵G. Wang, C. R. Crawford, and W. A. Kalender, "Multi-row detector and cone-beam spiral/helical CT," *IEEE Trans. Med. Imaging* **19**, 817–821 (2000).